www.czasopisma.pan.pl PAN www.journals.pan.pl
Opto-Electronics Review 25 (2017) 103–109

Contents lists available at ScienceDirect

Opto-Electronics Review

journal homepage: http://www.journals.elsevier.com/opto-electronics review

Mid-wave infrared liquid crystal shutter for breathalyzer applications

W. Piecek[a,*], L. Jaroszewicz[a], E. Miszczyk[b], Z. Raszewski[a], M. Mrukiewicz[a], P. Kula[a], K. Jasek[a], P. Perkowski[a], E. Nowinowski-Kruszelnicki[a], J. Zieliński[a], J. Kędzierski[a], M. Olifierczuk[a], U. Chodorow[a], P. Morawiak[a], R. Mazur[a], K. Kowiorski[c], P. Harmata[a], J. Herman[a]

[a] Military University of Technology (MUT), 00-908 Warsaw, Poland
[b] University of Technology and Humanities in Radom (UTH), 26-600 Radom, Poland
[c] Institute of Electronic Materials Technology, 01-919 Warsaw, Poland

ARTICLE INFO

Article history:
Received 23 January 2017
Received in revised form 17 March 2017
Accepted 17 March 2017
Available online 29 April 2017

Keywords:
Liquid crystal
Liquid crystal shutter
Breathalyzer
Infrared

ABSTRACT

There exists a problem with an in situ diagnostics of contamination of ethyl alcohol in a human being exhaled air. When ethyl alcohol in a mouth blowing (in a gaseous state) exists, the characteristic C—H stretch absorption bands in —CH_3 and —CH_2— functional groups in ethanol (CH_3—CH_2—OH) appear at a wavelength of $\lambda = 3.42$ μm. To investigate the presence of ethyl alcohol in exhaled human air, the light beam of $\lambda = 3.42$ μm is passing through an air sample. If one alternately measures the intensity of the investigated beam and the reference, a percentage of ethanol in the air sample can be estimated using a sensitive nondispersive infrared (NDIR) system with a stable operating flow mass detector. To eliminate a mechanical chopper and noise generating stepper motors, a photonic chopper as a liquid crystal shutter for $\lambda = 3.42$ μm has been designed. For this purpose, an innovative infrared nematic liquid crystal mixture was intentionally prepared. The working mixture was obtained by a selective removal of C—H bonds and its exchange by heavier polar substituents, what ensures a lack of absorption band of C—H bonds. The paper presents theory, concept and final experimental results of the infrared nematic liquid crystals mixture and the liquid crystal shutter for breathalyzer applications.

1. Introduction

There exists a problem with a rapid in situ diagnostics of contamination of ethyl alcohol in a human being exhaled air. When ethyl alcohol (EA) exists in a mouth blowing air the absorption bands characteristic for the stretch of C—H bonds existing in —CH_3 and —CH_2— functional groups of ethanol (CH_3—CH_2—OH), appear at a wavelength of $\lambda = 3.42$ μm. To investigate the presence of EA in the exhaled human air, the beam of $\lambda = 3.42$ μm is passing through air samples in a non dispersive infrared (NDIR) detector. Percentage of ethanol in these samples can be estimated by comparison of intensity of the investigated beam with the reference one. Therefore, our goal was to develop a liquid crystal shutter for breathalyzer applications which works at the wavelength of $\lambda = 3.4$ μm. To the best of author's knowledge, this is the first report on such device. It is a completely new idea. The liquid crystal shutter should satisfy the following restrictive requirements. In the absence of an electric field (at the OFF state) the transmission of an unpolarized beam t_{OFF} should be not smaller than 40%. When a driving voltage U, not higher than 30 V, is applied the transmission at ON state (t_{ON}) should be low enough to satisfy a requirement for contrast ratio (CR) which should be not less than 80:1. The frame time t which is the sum of switching-on t_{ON} and switching-off t_{OFF} times should be not larger than 125 ms. The above conditions for CR and t should be kept in a rather broad temperature range, from 10 to +45 °C. The working aperture of the device should be not less than 17 mm.

The liquid crystal shutter for $\lambda = 3.42$ μm (3.4LCS) developed at the Military University of Technology (MUT) presented in this paper is based on a single cell with a liquid crystalline layer of a thickness of $d \sim 15$ μm working at electrically controlled birefringence (ECB) mode. For assembling an empty 3.4LCS cell two substrates of fused silica quartz plates (QP) covered with porous indium tin oxide (PITO) electrodes transparent at $\lambda = 3.42$ μm, SiO_2 blocking films (BF) and rubbed polyimide alignment layers (PL) were sealed by standard technique used for manufacturing of liquid crystal displays (LCDs). The empty ECB cell was filled with an innovative InfraRed Nematic Liquid Crystals Mixture (IRLC) intentionally prepared for this purpose. The optical anisotropy of IRLC is $\Delta n \sim 0.12$ at $\lambda = 3.42$ μm. The working IRLC mixture was obtained by a selective removal of C—H molecular bonds and its exchange by

* Corresponding author.
E-mail address: wiktor.piecek@wat.edu.pl (W. Piecek).

https://doi.org/10.1016/j.opelre.2017.03.005
1896-3757/

heavier polar substituents, what ensures a lack of absorption at C—H band. In 3.4LCS (with $d \sim 15\,\mu m$ filled by IRLC with $\Delta n \sim 0.12\,\mu m$) for $\lambda = 3.42\,\mu m$, the limit ($2\Delta n \cdot d = \lambda$) for the appearing of the first interference maximum in an ECB effect is nearly satisfied ($3.60\,\mu m = 2\Delta n \cdot d \sim \lambda = 0.34\,\mu m$). Due to above, one obtained the liquid crystal shutter operating at $\lambda = 3.42\,\mu m$ and working at the temperature range from −10 to +45 °C. The 3.4LCS was successfully tested at the Military University of Technology, Warsaw, Poland.

2. Theory and concept of 3.42LCS

At the beginning of designing the breathalyzer liquid crystals' shutter we need to consider two well-known electro-optical effects. In the first step, let us assume that linearly polarized light of the wavelength λ enters the conventional cell with a twisted nematic (TN) structure (with twist angle $\Theta = \pi/2$). The plane of polarization of this light is perpendicular to the average molecular direction of rod-like molecules (director **n**) at the entrance of TN. The liquid crystal layer of the thickness d and the transmission axis of an "ideal" analyzer is parallel to the director **n** at the exit surface of the TN cell. Under those circumstances, the theoretical value of the transmission T_T of the TN cell can be given by the following expression [1]:

$$T_T = 1 - \frac{\sin^2\left((\pi/2)\sqrt{1 + \left((2d\Delta n/\lambda)\right)^2}\right)}{1 + \left(2d\Delta n/\lambda\right)^2}. \tag{1}$$

The maximum transmission T_T of the TN cell described above, operating at so-called "positive TN mode" appear when the following condition is valid:

$$\frac{2d\Delta n}{\lambda} = \sqrt{4k^2 - 1}, \tag{2}$$

where Δn is the optical anisotropy at the wavelength λ for the applied liquid crystal and $k = 1, 2, 3, \ldots$, describes the order of interference maximum in the TN cell.

Switching-on time t_{ON} and switching-off time t_{OFF} of the TN structure under the driving voltage U are defined by the following equations [2,3]:

$$t_{ON} \propto \frac{\gamma d^2}{\varepsilon_o \Delta\varepsilon U^2 - \pi^2 K_{TN}}, \quad t_{ON} \propto \frac{\gamma d^2}{\varepsilon_o \Delta\varepsilon U^2 - \pi^2 K_{TN}}, \tag{3}$$

where ε_0 is the electric permittivity of free space, $\Delta\varepsilon$ is the dielectric anisotropy and γ is the rotational viscosity of a liquid crystal. The factor K_{TN} describes elasticity of the structure for the complex deformation from the twisted to the HomeoTropic (HT) structure. This reduced elastic coefficient K_{TN} is expressed by splay (K_{11}), twist (K_{22}) and bend (K_{33}) elastic constants by [4]:

$$K_{TN} = K_{11} + \frac{1}{4}(K_{33} - 2K_{22}). \tag{4}$$

The second considered electro-optical effect is the electrically controlled birefringence (ECB) mode. At this mode, the beam of linearly polarized light of the wavelength λ enters normally the cell with the HomoGenous (HG) nematic structure and the plane of polarization of this light forms the angle $\alpha = +45°$ with the molecular director **n** of a birefringent HG layer of the thickness d. The transmission axes of the "perfect" analyzer forms the angle $\beta = -45°$ with **n**. The theoretical value of the transmission T_T of this HG cell placed between two crossed polarizers can be given by [5]:

$$T_T = \sin^2\left(\frac{\pi d\Delta n}{\lambda}\right). \tag{5}$$

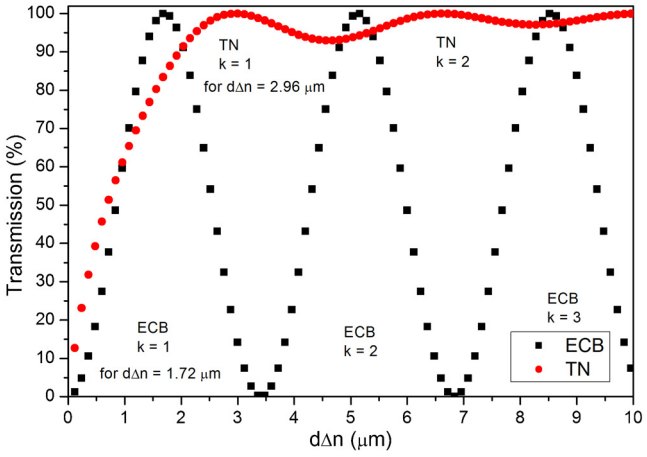

Fig. 1. Calculated values of theoretical transmissions T_T versus the $d\Delta n$ factor at the wavelength $\lambda = 3.42\,\mu m$ at TN and ECB operation modes.

The maximums of transmission T_T of the above, so-called "electrically controlled birefringence (ECB) – positive mode", appear when the following condition is fulfilled:

$$\frac{2d\Delta n}{\lambda} = 2k - 1, \tag{6}$$

where Δn is the optical anisotropy at λ for applied LC and $k = 1, 2, 3, \ldots$ describes the order of interference maximum in the ECB effect.

Switching-on time t_{ON} and switching-off time t_{OFF} at the ECB operating mode under driving voltage U are defined as follows:

$$t_{ON} = \propto \frac{\gamma d^2}{\varepsilon_o \Delta\varepsilon U^2 - \pi^2 K_{11}}, \quad t_{OFF} = \propto \frac{\gamma d^2}{\pi^2 K_{11}}. \tag{7}$$

Of course, the reduced elastic constant K_{11} is connected with the threshold voltage U_{th} of the liquid crystal deformation by the following formula:

$$U_{th} = \pi\sqrt{\frac{K_{11}}{\varepsilon_o \Delta\varepsilon}}. \tag{8}$$

Since in both TN and ECB effects switching-off times t_{OFF} are much higher than switching-on times t_{ON} [6], the total frame times $t = \tau_{ON} + \tau_{OFF}$ (which are the most crucial parameters for 3.4LCS) at the first approximation can be estimated as:

$$\text{for TN}: \quad t \approx t_{OFF} \propto \frac{\gamma d^2}{K_{TN}}, \tag{9}$$

$$\text{for ECB}: \quad t \approx t_{OFF} \propto \frac{\gamma d^2}{K_{11}} \tag{10}$$

In Fig. 1 calculated values of theoretical transmissions T_T versus the $d\Delta n$ factor for the chosen wavelength $\lambda = 3.42\,\mu m$ are presented. Here, the transmission T_T was computed on the base of Eq. (1) for TN and Eq. (6) for ECB effects, with an assumption that polarizers are "perfect".

Taking into account that the transmission coefficients τ of "real" polarizers: polarizer – P and analyzer – A are always smaller than 0.5 [7], one can evaluate the actual transmission T through 3.4LCS. If 3.4LCS it is armed with polarizer – P and analyzer – A of each transmission $\tau \sim 0.46$, the total transmission T via TN or ECB cells can be expressed by the equation [11]:

$$T = 2\tau^2 T_T \sim 0.42 T_T. \tag{11}$$

As to satisfy the main requirement for the 3.4LCS shutter on the total transmission T level, which should be higher than 40%, and taking the Eq. (11) into consideration, one can conclude that

the transmission T_T should be nearly 100%. Therefore, the 3.4LCS can be developed by utilizing both TN and ECB modes employing exactly the first ($k = 1$) maximum of interference (Fig. 1). In the ECB operation mode, the first maximum of interference appears at $d\Delta n = 1.72\ \mu m$ while in a TN one this maximum appears at $d\Delta n = 2.96\ \mu m$. Hence, the TN-based shutter will have a thickness d almost two times greater than the shutter based on the ECB operation mode. Due to Eqs. (9) and (10) and knowing that elastic constant K_{TN} is not more than two times higher than K_{11} [8,9] the frame time of ECB shutter should be two times shorter than this for TN one.

In the final analysis, to satisfy both technical requirements of 3.4LCS, taking into account the total transmission $T > 40\%$ and the frame time $t < 125$ ms, the transducer in the form of a single liquid crystal cell (LCC) of a rather high thickness $d \sim 15\ \mu m$ should be based on the ECB effect tuned into the first maximum of interference. To fill a cell with an intentionally synthesized liquid crystal material with the Mid-Wave InfraRed (MWIR) window was prepared.

3. InfraRed Nematic Liquid Crystal Mixture (IRLC) for 3.4LCS

InfraRed Nematic Liquid Crystal Mixture (IRLC) intentionally prepared for 3.4LCS should exhibit:

- mid-wave infrared absorption window with a bandwidth from approximately 3.2 μm to 3.7 μm,
- a positive value of both optical Δn and dielectric $\Delta\varepsilon$ anisotropies

$$\Delta n = n_e - n_o, \quad \Delta\varepsilon = \varepsilon_{||} - \varepsilon_{\perp}, \tag{12}$$

where n_e and n_o are extraordinary and ordinary refractive indices while, $\varepsilon_{||}$ and $\varepsilon_{\perp}$ are the parallel and perpendicular components of electric permittivity tensor ε,

- as high as possible the K_{11} elastic constant,
- as high as possible the optical Δn (for $\lambda = 3.42\ \mu m$) and dielectric $\Delta\varepsilon$ anisotropies,
- as small as possible rotational viscosity γ.

Due to our experiences [8,10–13] we established a new IRLC mixture for 3.4LCS application, abbreviated also W1973.

At the mid-wave infrared (MIR) region (from 3 μm to 5 μm) several molecular vibration bands are present, i.e. those characteristics for systems like CH, CH_2, CH_3, CN and NCS which are commonly found in mesogenic molecules. The strong absorption peak of a cyano group (CN) occurs at ~4.48 μm and isothiocyanato (NCS) polar group has a broad and strong absorption at the 4.5–5.2 μm band. Due to high anharmonicity of vibrations of CH, CH_2, CH_3 groups, the respective absorption bands are very strong and overlap closely and are centered at c.a. ~3.4 μm with a bandwidth from 3.2 μm to 3.7 μm. An example of the absorption spectrum characteristics for an exemplary liquid crystal mixture LCM (abbreviated also W1892) one can see in Fig. 2. Of course, such an "ordinary" LCM cannot be used for the construction of the desired shutter for the exhaled air analyzer because CH stretching absorption bands of CH_3 and CH_2 functional groups lie in the same place where the spectrum of ethanol (Fig. 3) being a subject of the analysis exists.

The molecular vibration frequency ω depends on the elastic constant κ and reduced mass μ of the diatomic oscillator according to the relation:

$$\omega \propto \sqrt{\frac{\kappa}{\mu}}. \tag{13}$$

As the reduced mass increases, the vibration frequency decreases and respective absorption band shifts toward a longer wavelength. To ensure a low absorption at the desired MIR window one needs to shift the absorption band further out to the longer wavelength IR region. To do this one needs to substitute hydrogen with a heavier atom such as fluorine. To prove such a concept of the elimination of LC slab's absorption band of the band characteristics for ethanol a perdeuterated (>99% D) 5CB (4′-pentylbiphenyl-4-carbonitrile) compound, abbreviated D5CB, was synthesized [14–16]. The carbon-deuteron (CD) absorption peak was shifted from band (3.5 μm) characteristics for CH group to the longer wavelength of 4.6 μm. Moreover, at both the NIR (0.75–3 μm) and MIR (8–12 μm) off-resonance regions, the D5CB presents the much clean absorption spectrum and much lower absorption coefficient than the parent nematogen 5CB. Simultaneously, other physical properties such as phase transition temperatures and birefringence remain near unchanged.

The IRLC mixture was characterized by several experimental methods. The phase transitions temperatures of IRLC were measured by using the polarizing microscope technique (POM). The polarizing microscope equipped with the hot stage was used. The investigated material has got the following phase sequence:

Cr : −12.0°C/N : +48.6°C/Iso.

Dielectric measurements of IRLC were performed using Impedance Analyzer HP 4192A with the measuring frequencies from 100 Hz to 10 MHz. The temperature characteristics of real parts of isotropic $\varepsilon_I(T)$, perpendicular $\varepsilon_{\perp}(T)$ and parallel $\varepsilon_{||}(T)$

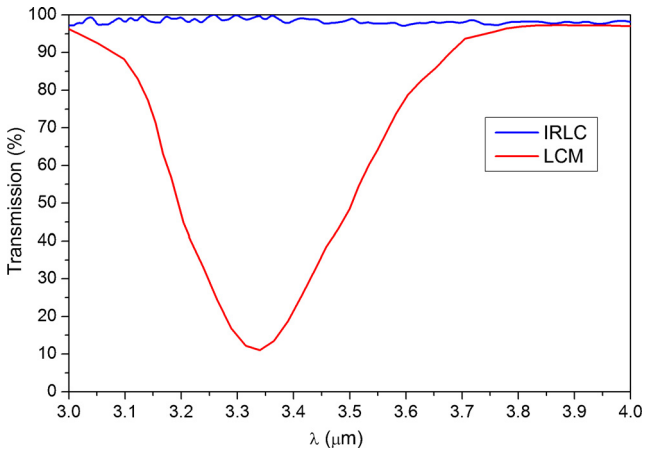

Fig. 2. Measured transmission spectra of LCM and IRLC in a mid-wave infrared region from 3.0 μm to 4.0 μm.

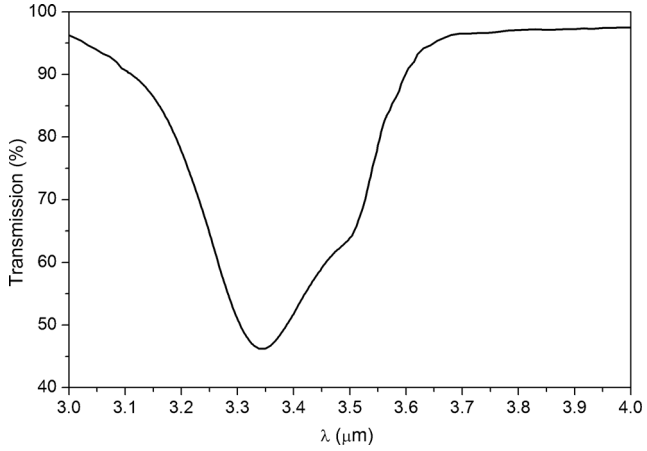

Fig. 3. Transmission spectra of ethanol (C_2H_5OH) in a mid-wave infrared region from 3.0 to 4.0 μm.

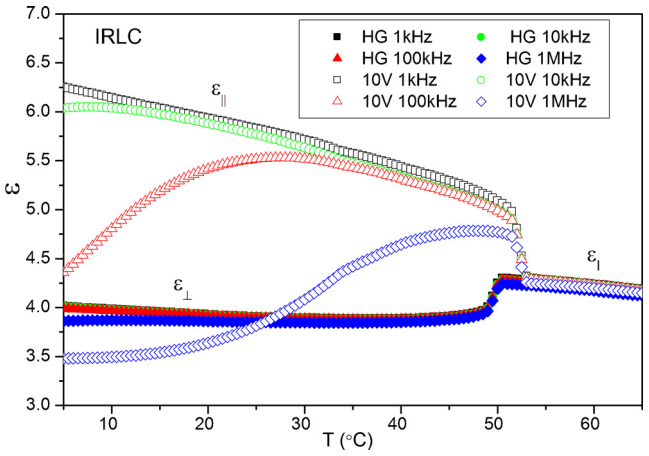

Fig. 4. Temperature dependence of $\varepsilon_{||}(T)$ and $\varepsilon_{\perp}(T)$ for IRLC measured at a frequency of 1, 10, 100 kHz and 1 MHz. The points of $\varepsilon_{||}(T)$ and $\varepsilon_{\perp}(T)$ were obtained by using the 4.9 μm thick HG cell with gold electrodes.

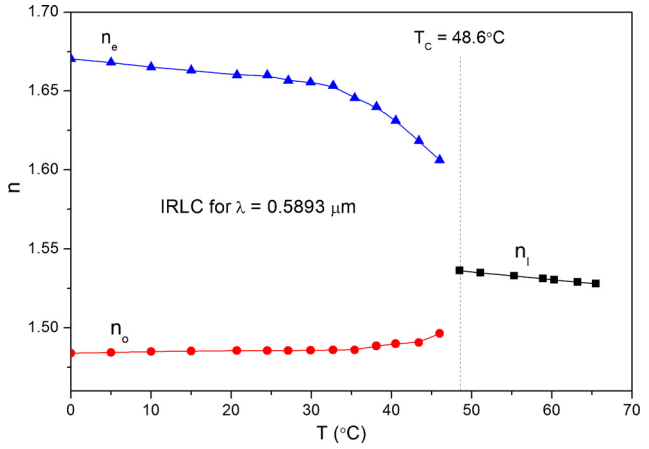

Fig. 5. Temperature dependence of $n_e(T)$ and $n_o(T)$ for IRLC at the yellow sodium line λ = 0.5893 μm. All points come from the Abbe refractometer.

components of electric permittivity tensors ε of IRLC were measured at nematic and isotropic phases. For this purpose, the HG measuring cell with the golden (Au) electrodes of active area $S = 5.08\ \text{mm} \times 5.08\ \text{mm}$ and cell gap $d = 4.9\ \mu\text{m}$ was used [17–19]. Low DC-field ($U = 10\ \text{V}$) was applied to the cell to switch molecular orientation from HG to the HT alignment. It allows calculating a dielectric anisotropy of $\Delta\varepsilon$ value. Temperature was stable within 0.2 K. The temperature characteristics of components $\varepsilon_{\perp}(T)$, $\varepsilon_{||}(T)$ and $\varepsilon_I(T)$ for IRLC are shown in Fig. 4.

Optical measurements of IRLC were performed using combined methods, applying appropriately prepared Abbe refractometer, wedged cells and interference methods [20,21]. The temperature characteristics of refractive indices $n_I(T)$, $n_o(T)$ and $n_e(T)$ were obtained by Abbe refractometer and wedged cells measurements at the yellow sodium line λ = 0.5893 μm (Fig. 5). When the HG cell of the cell gap d with IRLC is placed between crossed polarizers the birefringent interference fringes are recorded by the spectrometer in the wavelength domain λ (Fig. 6). The order k of a birefringent line at λ_k (λ_k is wavelength at the maximum of the birefringent fringe) is connected with the optical anisotropy $\Delta n(\lambda_k)$ and thickness d of the applied cell by the equation:

$$\Delta n(\lambda_k) = (2k-1)\frac{\lambda_k}{2d}. \tag{14}$$

Knowing the values of $n_e(\lambda)$ and $n_o(\lambda)$ from combined methods, applying both appropriately prepared Abbe refractometer and

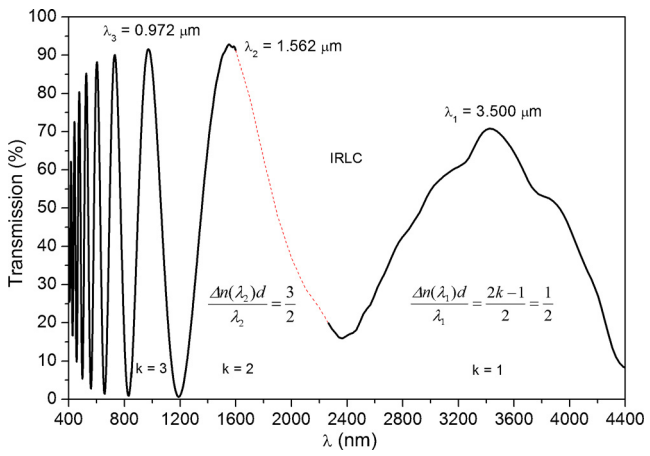

Fig. 6. The birefringent interference fringes of IRLC at 25 °C in a 6.3 μm thick HG cell placed between crossed polarizers. The spectra $T(\lambda)$ were recorded by JASCO V670 and BRUKER TENSOR 27 spectrometers.

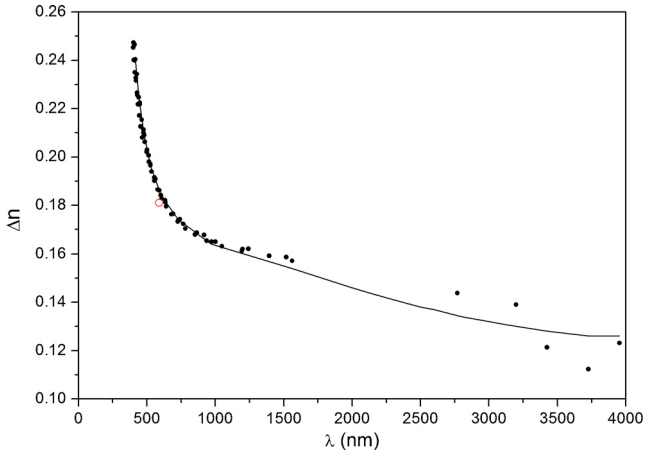

Fig. 7. Dispersion of the optical anisotropy $\Delta n(\lambda)$ for IRLC at 25 °C. The points marked by full circles come from interference methods. The solid line point marked by the red open circle comes from Abbe refractometer.

interference wedges (see Fig. 5) and being supported by interference methods (Fig. 6), the dispersion curve of optical anisotropy $\Delta n(\lambda)$ at 25 °C for IRLC was drawn (Fig. 7).

The measurements of the splay K_{11} elastic constant was based on determining threshold U_{th} voltage in a HG cell [22,23]. Fig. 8 shows the Freedericksz transition in the HG cell of the 4.9 μm cell gap. The HG cell with IRLC mixture was under the action of the voltage U and monitored during dielectric measurements. When dielectric anisotropy $\Delta\varepsilon > 0$ and threshold voltage U_{th} of IRLC are known, the splay K_{11} elastic constant can be calculated (Eq. (8) and Fig. 8).

Rotational viscosity $\gamma \approx 150\ \text{mPa s}$ of IRLC with $\Delta n \approx 1.7$ ($T = 25\ ^\circ\text{C}$, $\lambda = 0.5893\ \mu\text{m}$) was estimated from measurements of switching-off time $t_{OFF} \approx \tau_{100-10} \approx 4\ \text{ms}$ and switching-on time $t_{ON} \approx \tau_{0-90} \approx 1\ \text{ms}$ in the HG cell ($d = 1.8\ \mu\text{m}$) tuned to the first interference maximum at $\lambda = 0.5893\ \mu\text{m}$. An AC driving pulse of a square shape of amplitude $U = 20\ \text{V}$ was applied. Switching-on time t_{ON} and switching-off time t_{OFF} of a HG structure are defined by the Eq. (7).

The above measurements show that the frame time ($t = 110\ \text{ms}$) which is the sum of switching on t_{ON} and switching-off t_{OFF} times of the HG cell of thickness $d = 15.1\ \mu\text{m}$ (tuned to the first maximum interference for $\lambda = 3.42\ \mu\text{m}$) filled with IRLC (with $\Delta n \approx 1.2$ at $\lambda = 3.42\ \mu\text{m}$, $T = 25\ ^\circ\text{C}$) driven by nominated voltage $U = 30\ \text{V}$ is

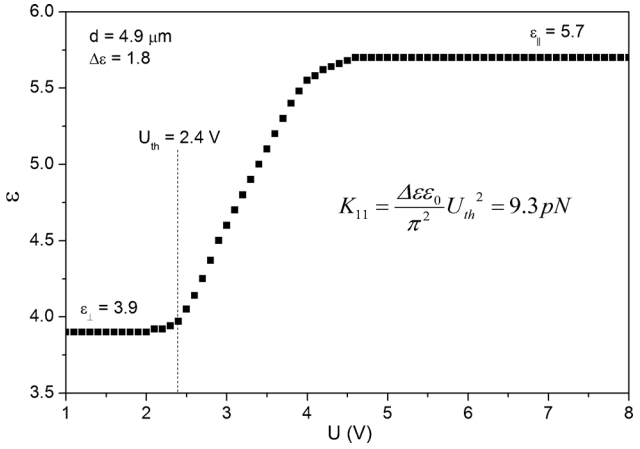

Fig. 8. Splay (K_{11}) deformation. Freedericksz transition of IRLC structure at 25 °C in a HG cell of 4.9 μm cell gap under voltage U monitored by dielectric measurements at f = 1.0 kHz.

Table 1
Material data of IRLC for 3.4LCS.

Material data	T = 25 °C	T = 40 °C
Perpendicular component $\varepsilon_\perp$ at: f = 1.0 kHz	3.9	3.9
Dielectric anisotropy $\Delta\varepsilon$ for: f = 1.0 kHz	1.8	1.6
Ordinary refractive index n_o for:		
λ = 0.589 μm	1.485	1.490
λ = 1.063 μm	1.446	1.448
λ = 3.420 μm	1.430	1.433
Optical anisotropy Δn for:		
λ = 0.589 μm	0.172	0.170
λ = 1.063 μm	0.135	0.131
λ = 3.420 μm	0.122	0.111
Absorption A of 15 μm layer of IRLC at λ = 3.420 μm	A < 2%	A < 2%
Threshold voltage U_{th} for splay deformation	U_{th} = 2.40 V	U_{th} = 2.35 V
Elastic constant K_{11} for splay deformation	9.3 pN	7.9 pN
Rotational viscosity γ	150 mPa s	130 mPa s

smaller than the wanted one (t < 125 ms) for 3.4LCS. The main material parameters of IRLC are gathered in Table 1.

4. Liquid crystal shutter for λ = 3.42 μm (3.4LCS)

Liquid crystal shutter for λ = 3.42 μm was based on a single ECB cell with rather a high cell gap of $d \sim 15$ μm. The layout of 3.4LCS with its main dimensions is given in Fig. 9.

To increase transmission T of as to excess of 40% one needs to minimize or remove some sources of transmitted light losses which appear in a simple glass used in the ECB or TN cell [11,12]. To achieve this aim 3.4LCS with T > 40% was constructed as a sandwich of different functional layers. The schematic cross section of 3.4LCS is shown in Fig. 10.

To reduce absorptions A_S of substrates of the ECB cell, fused silica (JGS3) windows, further called quartz plates (QP), of thickness d = 1.5 mm and $n \sim 1.45$ at λ ~ 3.4 μm [24] were applied. Due to $n \sim 1.45$ at λ ~ 3.4 μm the measured transmission T = 93.0% at λ = 3.4 μm of "clean" QP (Fig. 11) is nearly the same as the theoretical value (93.7% [11]), QP can be regarded as no absorptive ($A_S \sim 0$) ones.

To minimize light diffusion A_{LD} at boundary surfaces of quartz plates, both sides of QP were mechanically polished with an optical quality. After this, the flatness of QP was better than Lambda/62@633 nm and a wedge-shaped character of QP was smaller than 8″. The absorption A_{PL} of 30 nm of the applied polyimide aligning SE-130 layer is practically unmeasured one. To avoid a direct electrical contact of transparent PITO electrodes with sheet resistance 1600 Ω/sq (PITO1600) of a clean aperture

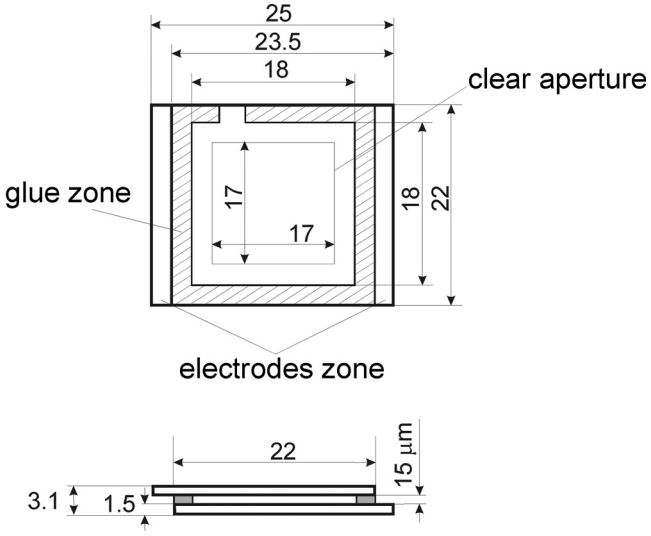

Fig. 9. Layout of 3.4LCS. Dimensions are in millimeters.

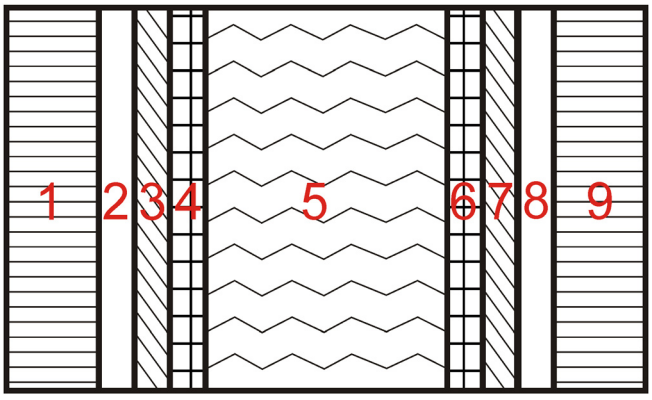

Fig. 10. The cross-section of 3.4LCS. 1 and 9 are Quartz Plates (QP); 2 and 8 are transparent porous indium tin oxide (PITO) layers; 3 and 7 are SiO_2 blocking films (BF); 4 and 6 are polyimide homogeneous alignment layers Nissan SE-130 (PL); 5 is IRLC.

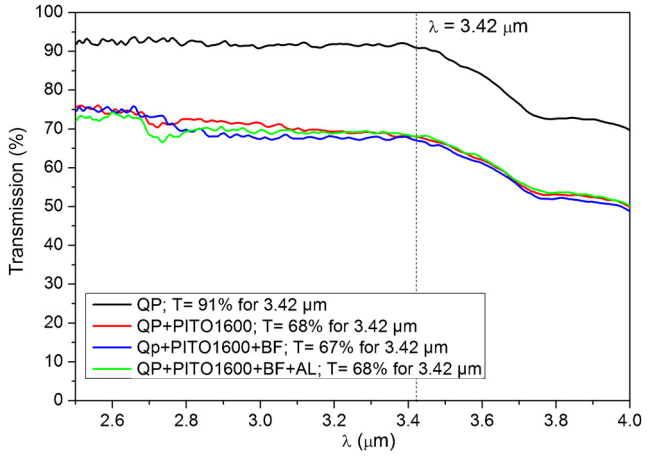

Fig. 11. Transmission spectra T as functions of wavelength λ of QP; QP with PITO1600; QP with PITO1600 and BF; QP with PITO1600, BF and AL.

(17 mm × 17 mm), the SiO_2 blocking film (BF) was evaporated on the PITO1600 layer. Transmissions spectra for quartz plates with all layers are presented in Fig. 11.

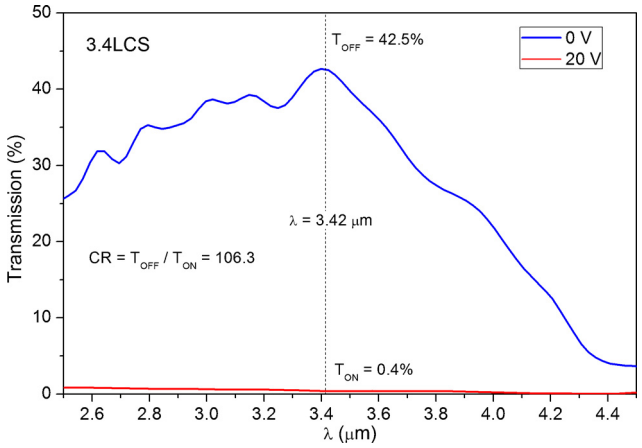

Fig. 12. The total transmissions T of 3.4LCS placed between crossed polarizers: t_{OFF} in OFF state (at $U = 0$ V) and t_{ON} in ON state (at $U = 20$ V) versus wavelength λ of 3.4LCS with thickness $d = 14.3$ μm. 3.4LCS was filled by IRLC (at $\Delta n \sim 0.12$ for $\lambda = 3.42$ μm at 25 °C).

Two QP substrates covered with PITO1600, BF and PL layers followed by a suitable rubbing (for induction an ECB effect) were sealed by standard operations of LCD technology [11,12]. The empty ECB cell was filled with an innovative nematic liquid crystals mixture (IRLC) with $\Delta n \sim 0.12$ at $\lambda \sim 3.4$ μm. The filling process was carried out in the LCD vacuum chamber at 25 °C. Due to above, one obtained the liquid crystal shutter for $\lambda = 3.42$ μm (3.4LCS) at the working temperature range from −10 to +45 °C.

Fig. 12 presents the transmissions t_{OFF} at the OFF state ($U = 0$ V) and t_{ON} at the ON state ($U = 20$ V) versus wavelength λ of 3.4LCS (with thickness $d = 14.3$ μm filled with IRLC, $\Delta n \sim 0.12$ μm at $\lambda = 3.42$ μm) at 25 °C placed between crossed polarizers. Both transmissions were obtained for 3.4LCS when the plane of polarization of incident light forms the angle of $\pi/4$ with the molecular director **n** at the entrance of IRLC layer. Both t_{ON} and t_{OFF} types of characteristics presented in Fig. 12 were measured by means of BRUKER TENSOR 27 Spectrophotometer equipped with IR ZnSe Polarizers. It can be seen that the maximum transmission t_{OFF} in OFF state lies exactly to $\lambda = 3.42$ μm. It indicates that the transition band of 3.4LCS is very well tuned to the work in the first interference maximum of ECB mode. In Fig. 12 one can notice not significant (~1%) "interference fingers" at the main ECB transmission t_{ON} and t_{OFF} curves of 3.4LCS. It means that 3.4LCS with IRLC working in both ON and OFF states can be regarded as the nearly refractive index matched liquid crystal cell. In the absence of an electric field (when $U = 0$ V) the transmission t_{OFF} (for $\lambda = 3.4$ μm of unpolarized light in OFF state) of 3.4LCS equipped with two crossed IR ZnSe Polarizers is (42.5%) higher than 40%. When the driving voltage of $U = 20$ V is applied, t_{ON} (in ON state) is 0.4% and then the requirement for contrast CR ~ 100% > 80%) is satisfied (when $U = 30$ V, CR ~ 200%).

5. Conclusions

3.4LCS with IRLC developed and manufactured by the Military University of Technology in Warsaw (Poland) were tested in the laboratories of MUT and UTH. The results of tests on 3.4LCS are gathered in Table 2. 3.4LCS with IRLC satisfy all technical requirements for dedicated breathalyzer applications.

Although 3.4LCS with IRLC satisfies all technical requirements for dedicated breathalyzer applications, the 3.4LCS is very slow one ($t = t_{ON} + t_{OFF} \sim 125$ ms when $U = 30$ V). In light of our research, it seems that it is possible to significantly lower frame time while reducing the control voltage. To do this one must develop a new IRLC mixture with optical the anisotropy Δn greater than 0.25 for at $\lambda \sim 3.4$ μm. Doubling the optical anisotropy Δn will double thickness d reduction ECB cell and then the frame time t will certainly fall below 50 ms under 20 V.

Table 2
The averaged (over amount of 3 items) results of investigations on 3.4LCS with IRLC.

No.	Type of test	Measured value
1	Thickness d of LCS	14.3 μm < d < 15.1 μm
2	Frame time $t = t_{ON} + t_{OFF}$ when $U = 30$ V	Not higher than 120 ms
3	Transmission t_{ON} at $\lambda = 3.4$ μm in ON state when $U = 20$ V	Not higher than 0.4%
4	Transmission t_{OFF} at $\lambda = 3.4$ μm in OFF state when $U = 0$ V	Not smaller than 41%
5	Contrast ratio	
	CR when $U = 20$ V	Not smaller than 100
	CR when $U = 30$ V	Not smaller than 200

Acknowledgements

This paper was done in 2016 under the financial support of the MUT University grant PBS 23-652 "Innovative materials and structures for photonics and electronics" and was partially supported by the National Science Center grant 2013/08/A/ST5/00773. The synthesis of Liquid Crystalline materials have been done under financial support from Polish National Science Centre Grant UMO-2012/05/D/ST5/03387.

References

[1] C.H. Gooch, H.A. Tarry, The optical properties of twisted nematic liquid crystal structures with twist angles ≤90 degrees, J. Phys. D: Appl. Phys. 8 (1975) 1575.
[2] K. Tarumi, U. Finkenzeller, B. Schuler, Dynamic behaviour of twisted nematic liquid crystals, Jap. J. Appl. Phys. 31 (1992) 2829–2836.
[3] H. Hirschmann, V. Reiffenrath, D. Demus, J. Goodby, G.W. Gray, H.-W. Spiess, V. Vill, Applications, TN, STN Displays, in: Handbook of Liquid Crystals Set, Wiley-VCH Verlag GmbH, 1998, pp. 199–229.
[4] R. Stannarius, D. Demus, J. Goodby, G.W. Gray, H.-W. Spiess, V. Vill, Elastic Properties of Nematic Liquid Crystals, in: Handbook of Liquid Crystals Set, Wiley-VCH Verlag GmbH, 1998, pp. 60–90.
[5] P. Yeh, C. Gu, Optics of Liquid Crystal Displays, 2 ed., Wiley, Hoboken, NJ, 2009.
ccurfalse
[3] H. Hirschmann, V. Reiffenrath, D. Demus, J. Goodby, G.W. Gray, H.-W. Spiess, V. Vill, Applications, TN, STN Displays, in: Handbook of Liquid Crystals Set, Wiley-VCH Verlag GmbH, 1998, pp. 199–229.
[4] R. Stannarius, D. Demus, J. Goodby, G.W. Gray, H.-W. Spiess, V. Vill, Elastic Properties of Nematic Liquid Crystals, in: Handbook of Liquid Crystals Set, Wiley-VCH Verlag GmbH, 1998, pp. 60–90.
[5] P. Yeh, C. Gu, Optics of Liquid Crystal Displays, 2 ed., Wiley, Hoboken, NJ, 2009.
[6] L. Jaroszewicz, Z. Raszewski, W. Piecek, P. Perkowski, E. Nowinowski-Kruszelnicki, Liquid Crystal Light Modulators, Bel Studio, Warsaw, 2014.
[7] D.N. Clarke, Polarized Light and Optical Measurement: International Series of Monographs in Natural Philosophy, Pergamon, 2013.
[8] E. Nowinowski-Kruszelnicki, J. Kędzierski, Z. Raszewski, L. Jaroszewicz, R. Dabrowski, M. Kojdecki, W. Piecek, P. Perkowski, K. Garbat, M. Olifierczuk, M. Sutkowski, K. Ogrodnik, P. Morawiak, E. Miszczyk, High birefringence liquid crystal mixtures for electro-optical devices, Opt. Appl. 42 (2012) 167–180.
[9] E. Nowinowski-Kruszelnicki, J. Kędzierski, Z. Raszewski, L. Jaroszewicz, M.A. Kojdecki, W. Piecek, P. Perkowski, M. Olifierczuk, E. Miszczyk, K. Ogrodnik, P. Morawiak, Measurement of elastic constants of nematic liquid crystals with use of hybrid in-plane-switched cell, Opto-Electron. Rev. 20 (2012) 255–259.
[10] Z. Raszewski, W. Piecek, L. Jaroszewicz, R. Dabrowski, E. Nowinowski-Kruszelnicki, L. Soms, M. Olifierczuk, J. Kędzierski, P. Morawiak, R. Mazur, E. Miszczyk, M. Mrukiewicz, K. Kowiorski, Transparent laser damage resistant nematic liquid crystal cell "LCNP3", Opto-Electron. Rev. 22 (2014) 196–200.
[11] Z. Raszewski, W. Piecek, L. Jaroszewicz, L. Soms, J. Marczak, E. Nowinowski-Kruszelnicki, P. Perkowski, J. Kędzierski, E. Miszczyk, M. Olifierczuk, P. Morawiak, R. Mazur, Laser damage resistant nematic liquid crystal cell, J. Appl. Phys. 114 (2013).
[12] E. Nowinowski-Kruszelnicki, L. Jaroszewicz, Z. Raszewski, L. Soms, W. Piecek, P. Perkowski, J. Kędzierski, R. Dabrowski, M. Olifierczuk, K. Garbat, E. Miszczyk, Liquid crystal cell for space-borne laser rangefinder to space mission applications, Opto-Electron. Rev. 20 (2012) 315–322.
[13] Z. Raszewski, E. Kruszelnicki-Nowinowski, J. Kędzierski, P. Perkowski, W. Piecek, R. Dabrowski, P. Morawiak, K. Ogrodnik, Electrically tunable liquid crystal filters, Mol. Cryst. Liq. Cryst. 525 (2010) 112–127.
[14] P. Kula, N. Bennis, P. Marć, P. Harmata, K. Gacioch, P. Morawiak, L.R. Jaroszewicz, Perdeuterated liquid crystals for near infrared applications, Opt. Mater. 60 (2016) 209–213.

[15] P. Kula, J. Herman, P. Harmata, M. Czerwiński, NIR and MWIR transparent liquid crystals, 2014 39th International Conference on Infrared, Millimeter, and Terahertz Waves (IRMMW-THz) (2014) 1–2, http://dx.doi.org/10.1109/IRMMW-THz.2014.6956108.
[16] Y. Chen, H. Xianyu, J. Sun, P. Kula, R. Dabrowski, S. Tripathi, R.J. Twieg, S.-T. Wu, Low absorption liquid crystals for mid-wave infrared applications, Opt. Express 19 (2011) 10843.
[17] Z. Raszewski, Measurement of permittivity of liquid-crystalline substances, Electron Technol. 20 (1987) 99–113.
[18] P. Perkowski, D. Łada, K. Ogrodnik, J. Rutkowska, W. Piecek, Z. Raszewski, Technical aspects of dielectric spectroscopy measurements of liquid crystals, Opto-Electron. Rev. 16 (2008) 271–276.
[19] P. Perkowski, Dielectric spectroscopy of liquid crystals. Theoretical model of ITO electrodes influence on dielectric measurements, Opto-Electron. Rev. 17 (2009) 180–186.
[20] J. Kędzierski, Z. Raszewski, M.A. Kojdecki, E. Kruszelnicki-Nowinowski, P. Perkowski, W. Piecek, E. Miszczyk, J. Zieliński, P. Morawiak, K. Ogrodnik, Determination of ordinary and extraordinary refractive indices of nematic liquid crystals by using wedge cells, Opto-Electron. Re, Opto-Electron. Rev. 18 (2010) 214–218.
[21] E. Miszczyk, Z. Raszewski, J. Kędzierski, E. Nowinowski-Kruszelnicki, M.A. Kojdecki, P. Perkowski, W. Piecek, M. Olifierczuk, Interference method for determining dispersion of refractive indices of liquid crystals, Mol. Cryst. Liq. Cryst. 544 (2011) 22–36.
[22] J. Kędzierski, M.A. Kojdecki, Z. Raszewski, J. Zieliński, L. Lipińska, Determination of anchoring energy, diamagnetic susceptibility anisotropy, and elasticity of some nematics by means of semiempirical method of self-consistent director field, SPIE Proceedings (2005), pp. 602305-1–602305-15.
[23] J. Kędzierski, M.A. Kojdecki, Z. Raszewski, P. Perkowski, J. Rutkowska, W. Piecek, L. Lipińska, E. Miszczyk, Composite method for determination of liquid crystal material parameters, Mol. Cryst. Liq. Cryst. Sci. Technol. Sect. A Mol. Cryst. Liq. Cryst. 352 (2000) 77–84.
[24] Quarzglas für die Optik, Daten und Eigenschaften, 2009.